References

[1]Adler, F. P., "Missile Guidance by Three-Dimensional Proportional Navigation," *Journal of Applied Physics*, Vol. 27, May 1956, pp. 500–507.

[2]Shinar, J., Rotsztein, Y., and Bezner, E., "Analysis of Three-Dimensional Optimal Evasion with Linearized Kinematics," *Journal of Guidance and Control*, Vol. 2, No. 5, 1979, pp. 353–360.

[3]Guelman, M., and Shinar, J., "Optimal Guidance Law in the Plane," *Journal of Guidance, Control, and Dynamics*, Vol. 7, No. 4, 1984, pp. 471–476.

[4]Cochran, J. E., No, T. S., and Thaxton, D. G., "Analytical Solutions to a Guidance Problem," *Journal of Guidance, Control, and Dynamics*, Vol. 14, No. 1, 1991, pp. 117–122.

[5]Guelman, M., "Closed Form Solution of True Proportional Navigation," *IEEE Transactions on Aerospace and Electronic Systems*, Vol. AES-12, July 1976, pp. 472–482.

[6]Yuan, P. J., and Chern, J. S., "Solutions of True Proportional Navigation for Maneuvering and Nonmaneuvering Targets," *Journal of Guidance, Control, and Dynamics*, Vol. 15, No. 1, 1992, pp. 268–271.

[7]Yuan, P. J., and Chern, J. S., "Ideal Proportional Navigation," *Journal of Guidance, Control, and Dynamics*, Vol. 15, No. 5, 1992, pp. 1161–1165.

Method for Improving Autopilot Lag Compensation in Intercept Guidance

Thomas R. Blackburn*

Hughes Missile Systems Company, Tucson, Arizona 85734-1337

Introduction

PROPORTIONAL guidance continues to be an important concept for intercept guidance. Practical, energy-efficient engagement transient properties are an important attribute. In its simplest form it is expressed as

$$a_c = \lambda V_c \dot{\varepsilon} \tag{1}$$

where a_c is commanded lateral acceleration, λ the guidance gain, V_c the closing velocity, and $\dot{\varepsilon}$ the inertial line-of-sight rate of the target with respect to the interceptor. Problems can arise in the intercept end game when autopilot lag becomes significant. This shortcoming was ameliorated with the intercept guidance quadratic optimal solution that represented the autopilot as a first-order lag.[1] Performance losses can still be exhibited when the autopilot is not well represented by a first-order lag. The development here presents an intercept guidance closed-form solution that mimics the energy-efficient command transient properties of idealized proportional guidance but accommodates linear autopilot models of arbitrary complexity.

Development

The proportional guidance law can also be expressed in the form[2]

$$a_c = \left(\lambda / t_g^2\right) M \tag{2}$$

where M is the zero-effort miss and t_g is time to intercept. This miss consists of

$$M = p_T - p_M \tag{3}$$

where p_T is the target predicted lateral position at the estimated intercept time (t_g). Here p_M is the vehicle response to its present state, commonly referred to as the zero-effort response. Acceleration profiles for proportional guidance assume the form[2]

$$a_c(t) = a_c(0)(1 - t/t_g)^{\lambda - 2}; \qquad 0 \le t \le t_g \tag{4}$$

Received July 31, 1995; revision received Nov. 15, 1995; accepted for publication Nov. 16, 1995.

*Senior Engineer Scientist, Guidance and Control Department, P.O. Box 11337. Senior Member AIAA.

Let $f(t)$ represent the interceptor position impulse response to commanded acceleration. The particular solution to the command history response must equal the predicted miss to make intercept. This requirement is expressed by the convolution integral

$$\int_0^{t_g} a_c(t_g - \tau) f(\tau)\,\mathrm{d}\tau = M \tag{5}$$

Substituting Eq. (4) into Eq. (5) and rearranging,

$$a_c(0) = \frac{t_g^{\lambda-2} M}{\int_0^{t_g} \tau^{\lambda-2} f(\tau)\,\mathrm{d}\tau} \tag{6}$$

The variable $a_c(0)$, (a_c) is available on each computing cycle (time zero) to set to satisfy this equation. Integration by parts in Eq. (6) yields

$$a_c = M/F; \qquad \lambda = 2 \tag{7}$$

$$a_c = \frac{t_g M}{t_g F - E}; \qquad \lambda = 3 \tag{8}$$

$$a_c = \frac{t_g^2 M}{2D - 2t_g E + t_g^2 F}; \qquad \lambda = 4 \tag{9}$$

where

$$F \triangleq \int_0^{t_g} f(\tau)\,\mathrm{d}\tau \tag{10}$$

$$E \triangleq \int_0^{t_g} F(\tau)\,\mathrm{d}\tau \tag{11}$$

$$D \triangleq \int_0^{t_g} E(\tau)\,\mathrm{d}\tau \tag{12}$$

Equations (7–9) can be consolidated into

$$a_c = \frac{t_g^{\lambda-2} M}{\left\{(\lambda-2)\left[(\lambda-3)D - t_g^{\lambda-3}E\right] + t_g^{\lambda-2}F\right\}} \tag{13}$$

for a λ of 2, 3, or 4.

Define

$$\lambda^*(\lambda, t_g) \triangleq \frac{t_g^{\lambda}}{\left\{(\lambda-2)\left[(\lambda-3)D - t_g^{\lambda-3}E\right] + t_g^{\lambda-2}F\right\}} \tag{14a}$$

$$\lambda = 2, 3, 4 \tag{14b}$$

Then, substitution into Eq. (13) yields

$$a_c = \left(\lambda^*/t_g^2\right) M \tag{15}$$

and λ^* can be used interchangeably with λ in Eq. (1) or Eq. (2). Expression (14) is the central contribution of this Engineering Note. It will be referred to as profiled guidance in the following discussion.

Bryson[3] has shown that, assuming a vehicle model has no command-response lag, proportional guidance with a gain of three is optimal. The profiled solution assuming a λ of 3 is therefore of the most interest and is developed further.

Example 1

The profiled solution will now be applied to the system with the first-order-lag autopilot defined by the Laplace form

$$f(s) = \frac{1}{s^2(1 + Ts)} \tag{16}$$

and compared with the optimal[1] solution.

The impulse response of this system is

$$f(t) = Te^{-t/T} + t - T \tag{17}$$

Integrating Eq. (17) yields

$$F(t) = -T^2 e^{-t/T} + (t^2/2) - Tt + T^2 \tag{18}$$

A second integration of Eq. (17) yields

$$E(t) = T^3 e^{-t/T} + (t^3/6) - T(t^2/2) + T^2 t - T^3 \tag{19}$$

Substituting Eqs. (18) and (19) into Eq. (14) yields

$$\lambda^* = \frac{r^3}{[(r^3/3) - (r^2/2) + 1 - (1+r)e^{-r}]} \tag{20}$$

where

$$r \triangleq t_g/T \tag{21}$$

For comparison, the optimal gain[1] has the solution

$$\tilde{\lambda} = (e^{-r} + r - 1) \Bigg/ \left(\frac{r^2}{2} e^{-2r} + \frac{2}{r} e^{-r} - \frac{r}{3} + 1 - \frac{1}{r} - \frac{1}{2r^2} \right) \tag{22}$$

The zero-effort response is given by

$$p_M = p + t_g v + (e^{-r} + r - 1) T^2 a \tag{23}$$

where p, v, and a are vehicle present position, velocity, and acceleration. Figure 1 shows the command profiles for the profiled and optimal schemes. Notice that the Optimal guidance provides a commanded-acceleration profile slightly different from that of proportional guidance with a navigation constant (λ) of 3, as defined by Eq. (4), but the profiled guidance matches it exactly. Figure 2 shows the gain histories of the two schemes. The profiled gain is slightly lower than the optimal.

Example 2

The setup and transients were repeated with the second-order autopilot model expressed in Laplace form:

$$f(s) = \frac{\omega^2}{s^2(s^2 + 2\zeta\omega s + \omega^2)} \tag{24}$$

The impulse-response equation is

$$f(t) = t(2\alpha/\omega^2) + (e^{-\alpha t}/\beta)\sin(\beta t + 2\psi) \tag{25}$$

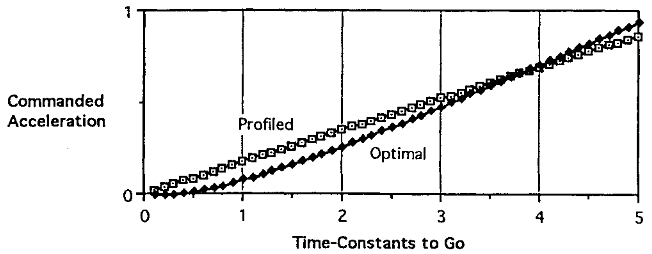

Fig. 1 First-order command response profiles.

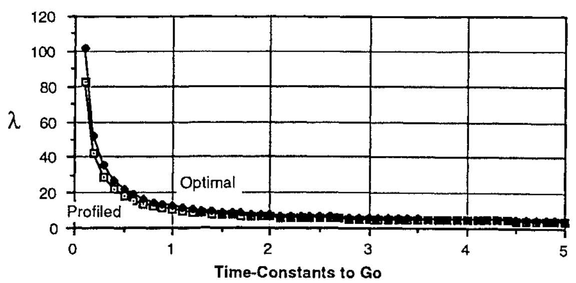

Fig. 2 First-order gain history comparison.

where

$$\alpha \triangleq \zeta\omega \tag{26}$$

$$\beta \triangleq \omega\sqrt{\zeta^2 - 1} \tag{27}$$

$$\psi \triangleq \tan^{-1}\sqrt{1/\zeta^2 - 1} \tag{28}$$

With two time integrations, one obtains

$$F(t_g) = \frac{1}{\beta\omega}\sin(3\psi) - 2\frac{\alpha}{\omega^2}t_g^2 + \frac{1}{2}t_g^2 - \frac{e^{-\alpha t_g}}{\beta\omega}\sin(\beta t_g + 3\psi) \tag{29}$$

and

$$E(t_g) = \frac{1}{\beta\omega}\sin(3\psi)t_g - \frac{\alpha}{\omega^2}t_g^2 + \frac{t_g^3}{6} + \frac{e^{-\alpha t_g}}{\beta\omega^2}\sin(\beta t_g + 4\psi) - \frac{1}{\beta\omega^2}\sin(4\psi) \tag{30}$$

Substituting Eqs. (29) and (30) into Eqs. (14) yields

$$\lambda^* = t_g^3 \Bigg/ \left\{ \frac{\alpha}{\omega^2}t_g^2 - \frac{1}{3}t_g^3 - \frac{1}{\beta\omega^2}\sin(4\psi) + \frac{e^{-\alpha t_g}}{\beta\omega^2}[\sin(\beta t_g + 4\psi) + \omega t_g \sin(\beta t_g 3\psi)] \right\} \tag{31}$$

The zero-effort response is

$$p_M = p + t_g v + \phi_3 a + \phi_4 \dot{a} \tag{32}$$

where

$$\phi_3 = \frac{2\alpha\omega^2 t_g + \beta^2 - 3\alpha^2}{\omega^4} + \frac{e^{-\alpha t_g}\sin(\beta t_g + 3\psi)}{\beta\omega} \tag{33}$$

$$\phi_4 = \frac{\omega^2 t_g - 2\alpha}{\omega^4} + \frac{e^{-\alpha t_g}\sin(\beta t_g + 2\psi)}{\beta\omega^2} \tag{34}$$

The first- and second-order autopilot models are matched with

$$\omega = 2\zeta/T \tag{35}$$

Figure 2 shows the profile-gain histories from the systems with the matched first- and second-order autopilots for comparison. The second-order gain history begins its sharp increase substantially before that for the first-order system, evidence that an adjusted gain history is appropriate for higher order autopilots. Notice that all of the gains of Figs. 2 and 3 converge to the proportional guidance gain of three with increasing time to go. Also important is the extra term in the zero-effort miss of Eq. (32) that includes the effect of vehicle acceleration (or rotation) rate in predicting miss.

The closed-form solutions obtained are limited to whole integers of the proportional guidance gain λ. Linear interpolation between the whole-integer solutions, however, has proven practical. We achieved the best simulated miss distance standard deviations at an interpolated gain of about 3.2. At this gain the simulated miss distance standard deviation was 14% smaller than that achieved with the referenced optimal guidance for our particular interceptor.

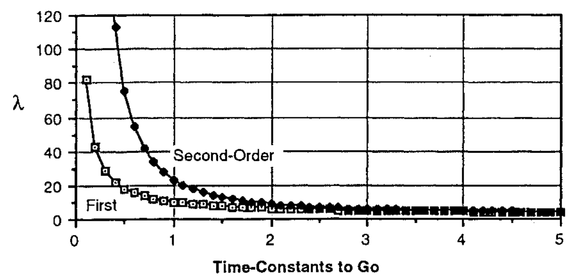

Fig. 3 Gain history comparison.

References

[1]Cottrell, R. G., "Optimal Intercept Guidance for Short Range Tactical Missiles," *AIAA Journal*, Vol. 9, No. 7, 1971, pp. 1414, 1415.

[2]Zarchan, P., *Tactical and Strategic Missile Guidance*, AIAA, Washington, DC, 1994, pp. 40, 42.

[3]Bryson, A. E., "Linear Feedback Solutions for Minimum Effort Interception, Rendezvous, and Soft Landing," *AIAA Journal*, Vol. 3, No. 8, 1965, pp. 1542–1544.

Passivity Motivated Controller Design for Flexible Structures

Declan Hughes* and John T. Wen†

Rensselaer Polytechnic Institute, Troy, New York 12180

I. Introduction

INHERENT passivity in fully actuated mechanical systems has long been recognized and exploited for their stabilization.[1] Even for underactuated systems, such as flexible robots, passivity remains a useful property. It has been shown that under an observability condition[2] strictly passive feedback between these passive pairs can render the closed-loop system asymptotically stable, even for an open-loop undamped system. When the input/output relationship is not passive, e.g., in the case of noncollocated actuator and sensor pairs, strictly passive feedback no longer guarantees stability. The purpose of this Note is to present some extension of the passivity approach to nonpassive input/output pairs through suitable incorporation of a nominal dynamical model of the system.

II. Nonpassive Input/Output Pairs

Controlled structures usually contain more sensors than actuators because of the weight and cost factors. As a result, the standard collocated feedback control can only utilize a subset of the sensors. Furthermore, some internal subspace may not be strongly observable from just sensors that are collocated with the actuators. It is possible to apply loop transformations to convert the nonpositive-real transfer functions (from inputs to the noncollocated outputs) by adding fictitious feedforwards and compensating for their effects with a feedback loop around the controller. The net result is a relatively small feedback gain and reduced gain and phase margins. For our physical experiment, in addition to the hub potentiometer, we have four strain gauges mounted on the beam (including one at the beam root next to the hub). The hub angle proportional-derivative (PD) feedback loop provides good rigid body mode response with little or no overshoot, approximately critically damps the first flexible mode, and offers good gain and phase margins. The higher order closed-loop flexible modes, however, remain relatively poorly damped. To provide additional damping to these flexible modes, we modify the PD feedback gains by closing a second feedback loop around the strain gauges. A direct PD feedback from the strain gauges requires small gains (the third and fourth strain gauges are nonminimum phase with respect to the torque input) and produces little improvement, or even degradation, in terms of closed-loop damping over the collocated (hub angle) loop. In this section, we shall present an alternative approach that is based on the observation that there is always some nominal model of the system via either analytic modeling or experimental identification, and it is possible to use this information to synthesize an approximately passive output. This approach consists of the following steps: Close all naturally passive loops using the procedure described in the preceding section; by using all of the outputs in an observer, estimate the full state of a reduced-order plant with the naturally passive loops closed; and synthesize an approximate passive output by passing the estimated full state through an output map D.

The preceding approach is a direct generalization of the naturally passive case, the only difference being that the passive output here is synthesized using an observer vs a physically available measurement in the previous case. It should be expected that the amount of performance improvement that can be provided by the outer loop depends on the modeling accuracy of the plant. Large modeling error would lead to reduced gain and bandwidth of the feedback controller.

There are two parameters that need to be selected in this design: 1) passive output map D that operates on the reconstructed full state and 2) observer feedback gain L. We have adopted a procedure to sequentially select these two parameters. The passive output map D is chosen based on the desired modal damping. After D is selected, the observer gain L is chosen based on the consideration of closed-loop transient response, actuator and sensor noises, and unmodeled dynamics.

Passive Output Map

The naturally passive loop can usually provide adequate damping for a number of modes. The nonpassive loop should be designed to add damping to other weakly damped modes. To selectively add damping into specified modes, we choose D based on the Lur'e equations, the solvability of which is a sufficient condition for strict positive realness[3]:

$$D = B^T P \tag{1}$$

$$A_c^T P + P A_c = -Q \tag{2}$$

The weighting matrix Q can be selected to be diagonal with entries corresponding to the desired modes emphasized. If the intercoupling between plant modes due to naturally passive output feedback is small (as is the case for poorly damped flexible modes) then a strong correlation is found between the magnitude of the diagonal elements of Q and the damping ratios of associated flexible modes when this negative feedback loop is added. This experience is justified in the ideal case (i.e., perfect model, noise free). Consider the quadratic Lyapunov function candidate $V(x) = \frac{1}{2}x^T Px$. The closed-loop system is governed by [with uncontrollable stable observable dynamics $D(sI - A + LC)^{-1}$ omitted for simplicity of presentation]

$$\dot{x} = A_c x + Bu \qquad y = Dx \qquad u = -Ky \tag{3}$$

where K, for simplicity, is chosen as a positive definite matrix (K is a positive real filter in general). The time evolution of V along the solution is then given by $\dot{V}(x) = -x^T Qx - y^T Ky \leq -x^T Qx$. Intuitively, if Q is diagonal, then increasing the entries corresponding to certain mode will increase its influence on the rate of decay of $\dot{V}(x)$. More specifically, the exponential decay rate of x is governed by the QP^{-1}. If P is approximately diagonal (as is the case for our experiment), then the entries of Q will have a direct influence on the damping of the corresponding modes.

Observer Feedback Gain

In the ideal case that the plant is exact and the noise can be neglected, the synthesized output y_{pr} is related to u by

$$Y_{pr}(s) = D(sI - A_c)^{-1}BU(s)$$

where A_c is the nominal system matrix with the naturally passive loop closed, $A_L \triangleq A_c - LC$, and $\hat{x}$ is the state estimate. Therefore, the first rule is: choose L so that the transient effect of $D(sI - A_L)^{-1}$ is small (i.e., place the poles of A_L beyond the desired closed-loop bandwidth).

In a real system, some unmodeled dynamics of the system with collocated loop closed are always present. We consider the

Received Sept. 3, 1993; revision received Oct. 6, 1995; accepted for publication Oct. 10, 1995.

*Ph.D. Student, Department of Electrical, Computer, and Systems Engineering; currently Research Associate, Department of Aerospace Engineering, Texas A&M University, College Station, TX 77843.

†Associate Professor, Control Laboratory for Mechanical Structures, Center for Advanced Technology in Automation, Robotics and Manufacturing, Department of Electrical, Computer, and Systems Engineering.